Beamforming Design for OFDM Joint Sensing and Communication System

Minggan Ye[1], Wei Hu[1], Yifeng Zhao[2*], Lianfen Huang[2], Zhiyuan Shi[1]

[1] Department of Electronic Science and Engineering, Xiamen University, China
[2] Department of Information and Communication Engineering, Xiamen University, China
23120201150210@stu.xmu.edu.cn, huwei@stu.xmu.edu.cn, zhaoyf@xmu.edu.cn, lfhuang@xmu.edu.cn, zyshi@xmu.edu.cn

Abstract

In this paper, we discussed the beamforming schemes for OFDM-based joint sensing and communication (OFDM-JSC) system, which enable JSC system to use directional beams to detect directions of interest, while communicating with one or more downlink users, thus further enhancing the practicability of JSC system. Specifically, we equip OFDM-JSC transmitter with hybrid beamforming structure and digital beamforming structure in SU-MIMO and MU-MISO scenarios, respectively. For SU-MIMO JSC, we separately considered the hybrid beamforming design with partially connected structure and fully connected structure. For MU-MISO JSC, we separately consider the beamforming design with total antenna array transmit power constraint, and per antenna transmit power constraint. For the four non-convex problems in above two scenarios, we have designed corresponding low-complexity JSC beamforming algorithms and we verified the effectiveness of proposed schemes through numerical simulation.

Keywords: Joint Sensing-and-Communication, OFDM, Beamforming, SU-MIMO, MU-MISO

1 Introduction

Since 5G communication [1] and mmWave radar [2] are tending to operate in the same frequency band, using the same equipment to achieve communication and sensing can effectively reduce hardware redundancy and power consumption, while avoiding electromagnetic interference, thereby improving spectrum utilization, which known as Joint Sensing-and-Communication (JSC), or Integrated Sensing-and-Communication (ISAC). To materialize JSC system, the integration of sensing and communication in waveform level should be first resolved [3]. The famous integrated sensing-and-communication waveform is OFDM [4]. Since JSC system acts as both base station (BS) and radar, the beamforming schemes solely for downlink communication or radar sensing will no longer work for it. Specifically, in order to improve radar sensing performance, it is desirable to concentrate limited transmit power in directions which need to be detected. However, if communication users are not located in detection directions, then downlink communication performance will suffer serious loss at this time. Conversely, if the beamforming in JSC transmitter only serves the downlink communication, the echo signal power in detection directions will be severely attenuated, especially when all users are NLOS. The simplest solution is to make JSC system emit an omnidirectional beam, or just serve users in detection directions, which means a waste of system resources. Furthermore, the communication and sensing services that JSC system needs to provide vary by scenario. Even in the same scenario, the communication and sensing requirements that JSC system needs to meet may change over time. At one moment, JSC system may need to communicate with more users, while at another moment, JSC system may need to detect more directions. Therefore, the beamforming design specifically for downlink communication or radar sensing will greatly reduce the comprehensive performance of JSC system.

In summary, the beamforming design for JSC system is a problem worthy of study. [5] proposes a beamforming scheme for JSC transmitter equipped with partially connected hybrid beamforming structure in SU-MIMO scenario, however, it is only for narrowband JSC system and its computational complexity is relatively high. [6] proposes a beamforming design for OFDM-JSC system, however it only focuses on designing transmit beampattern and does not consider the channel state information. [7-8] propose the beamforming design for JSC transmitter in MU-MISO scenario, and they both meet the sensing needs by unilaterally sacrificing a certain communication performance. [9-10] propose the beamforming design for JSC transmitter with analog beamforming structure, which can provide a wide field of view (FoV) for radar sensing. [11-13] provide a special solution, where both communication module and radar module use OFDM waveform, while communication signal and radar signal, as well as communication antenna and radar antenna, are independent of each other, which means the communication module needs to use additional digital precoding to offset the interference caused by radar signal. [14] introduces RIS to assist passive beamforming for narrowband JSC system in MU-MISO scenario. Here we propose a novel beamforming design for OFDM-JSC system to meet the changing needs of communication and sensing in actual scenarios by flexibly adjusting the weights assigned to downlink communication and radar sensing.

2 Hybrid Beamforming Design for SU-MIMO JSC

2.1 System Model

*Corresponding Author: Yifeng Zhao; E-mail: zhaoyf@xmu.edu.cn
DOI: 10.53106/160792642022122307001

We consider an OFDM-JSC system in single-user MIMO (SU-MIMO) scenario, whose transmitter equipped with N_t antennas ULA, and performs downlink communication with a UE whose receiver equipped with N_r antennas ULA. In the meantime, OFDM-JSC system senses the surrounding environment by pointing directional beams in N_{tar} directions of interest, and tracks the targets by receiving the echo signal. The OFDM-JSC transmitter adopts hybrid beamforming structure equipped with N_{RF} RF chains, and both fully connected structure and partially connected structure will be discussed separately in the following. While fully digital combining structure is considered in UE receiver, as shown in Figure 1.

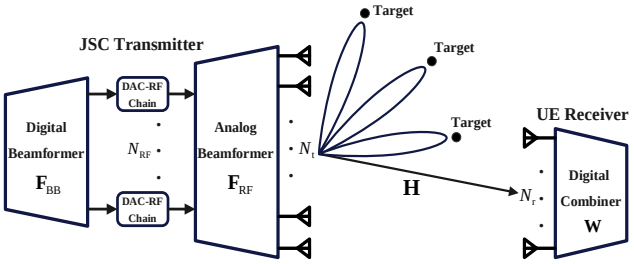

Figure 1. Hybrid JSC beamforming in SU-MIMO scenario

2.2 Communication Model

Assuming the OFDM integrated sensing-and-communication waveform [15] is used in above JSC system. After the baseband demodulation operation in UE receiver, the received symbol vector at kth subcarrier can be expressed as

$$\mathbf{y}[k]=\mathbf{W}^H[k]\mathbf{H}[k]\,\mathbf{F}_{\mathrm{RF}}\,\mathbf{F}_{\mathrm{BB}}[k]\mathbf{s}[k]+\mathbf{W}^H[k]\mathbf{n}[k]. \quad (1)$$

Where $k \in \mathcal{K} = \{1, \dots, K\}$ is the subcarrier index, and suppose there are K subcarriers in total. $\mathbf{s}[k] = \left[\mathrm{s}_1[k], \dots, \mathrm{s}_{N_\mathrm{s}}[k]\right]^T \in \mathbb{C}^{N_\mathrm{s}\times 1}$ denotes for the N_s data streams transmitted towards UE at kth subcarrier, which satisfies that $\mathbb{E}\{\mathbf{s}[k]\mathbf{s}^H[k]\} = \mathbf{I}_{N_\mathrm{s}}$. And to enable multi-stream communication, $N_\mathrm{s} \le N_{\mathrm{RF}} \le N_\mathrm{t}$ and $N_\mathrm{s} \le N_\mathrm{r}$ should also be satisfied. $\mathbf{n}[k] \in \mathbb{C}^{N_\mathrm{r}\times 1}$ represents the complex AWGN vector at kth subcarrier, whose elements satisfy independent and identically distribution $\mathcal{CN}(0, \sigma_n^2)$.

$\mathbf{F}_{\mathrm{BB}}[k] \in \mathbb{C}^{N_{\mathrm{RF}}\times N_\mathrm{s}}$ is the digital beamforming matrix for kth subcarrier and the fully digital combining matrix for kth subcarrier in UE receiver is represented by $\mathbf{W}[\mathrm{k}] \in \mathbb{C}^{N_\mathrm{r}\times N_\mathrm{s}}$. In fully connected hybrid beamforming (HBF) structure, all elements of the analog beamforming matrix $\mathbf{F}_{\mathrm{RF}} \in \mathbb{C}^{N_\mathrm{t}\times N_{\mathrm{RF}}}$ need to satisfy unit modulus constraint as $\left|(\mathbf{F}_{\mathrm{RF}})_{i,j}\right| = 1,\ i = 1, \dots, N_\mathrm{t},\ j = 1, \dots, N_{\mathrm{RF}}$.

While in partially connected hybrid beamforming (HBP) structure, each of RF chain is connected to a subarray consisting of $\frac{N_\mathrm{t}}{N_{\mathrm{RF}}}$ antennas. The corresponding analog beamforming matrix with block diagonal structure can be expressed as [16]

$$\mathbf{F}_{\mathrm{RF}} = \begin{bmatrix} \mathbf{r}_1 & \mathbf{0} & \cdots & \mathbf{0} \\ \mathbf{0} & \mathbf{r}_2 & & \mathbf{0} \\ \vdots & & \ddots & \vdots \\ \mathbf{0} & \mathbf{0} & \cdots & \mathbf{r}_{N_{\mathrm{RF}}} \end{bmatrix} \in \mathbb{C}^{N_\mathrm{t}\times N_{\mathrm{RF}}}. \quad (2)$$

$$\mathbf{r}_i = \left[\exp\left(\mathrm{j}\theta_{(i-1)\frac{N_\mathrm{t}}{N_{\mathrm{RF}}}+1}\right), \dots, \exp\left(\mathrm{j}\theta_{i\frac{N_\mathrm{t}}{N_{\mathrm{RF}}}}\right)\right]^T \in \mathbb{C}^{\frac{N_\mathrm{t}}{N_{\mathrm{RF}}}\times 1}, i = 1, \dots, N_{\mathrm{RF}},$$ and θ stands for the phase of corresponding phase shifter. And all non-zero entries of $\mathbf{F}_{\mathrm{RF}}$ should still satisfy unit modulus constraint.

It's worth to emphasize that in the hybrid beamforming structure, the analog beamforming matrix $\mathbf{F}_{\mathrm{RF}}$ is shared by all subcarriers, while the digital beamforming matrix $\mathbf{F}_{\mathrm{BB}}[k] \in \mathbb{C}^{N_{\mathrm{RF}}\times N_\mathrm{s}}$ is performed for each subcarrier [17]. Let P_T denotes the average transmit power per subcarrier, for the whole bandwidth we have the constraint $\sum_{k\in\mathcal{K}}\|\mathbf{F}_{\mathrm{RF}}\mathbf{F}_{\mathrm{BB}}[k]\|_F^2 = KP_T$. For partially connected hybrid beamforming structure, we can also draw the conclusion that $\sum_{k\in\mathcal{K}}\|\mathbf{F}_{\mathrm{BB}}[k]\|_F^2 = \frac{KN_{\mathrm{RF}}P_T}{N_\mathrm{t}}$.

$\mathbf{H}[k] \in \mathbb{C}^{N_\mathrm{r}\times N_\mathrm{t}}, k = 1, \dots, K$ denotes for the frequency domain channel matrix at kth subcarrier. Here we adopt the wideband SV channel model with N_C clusters and N_R rays within each cluster, which can be expressed as [17]

$$\mathbf{H}[k] = \sqrt{\frac{N_\mathrm{t}N_\mathrm{r}}{N_\mathrm{C}N_\mathrm{R}}}\sum_{i=1}^{N_\mathrm{C}}\sum_{j=1}^{N_\mathrm{R}}\alpha_{ij}\mathbf{a}_\mathrm{r}(\theta_{ij}^\mathrm{r})\mathbf{a}_\mathrm{t}(\theta_{ij}^\mathrm{t})^H e^{-\mathrm{j}\frac{2\pi}{K}(i-1)(k-1)}. \quad (3)$$

Where $\sqrt{\frac{N_\mathrm{t}N_\mathrm{r}}{N_\mathrm{C}N_\mathrm{R}}}$ is a normalization factor to guarantee $\mathbb{E}[\|\mathbf{H}[k]\|_F^2] = N_\mathrm{t}N_\mathrm{r}$. α_{ij} is the complex gain of jth ray in i th propagation cluster following complex Gaussian distribution $\alpha_{ij} \sim \mathcal{CN}(0,1)$. θ_{ij}^r and θ_{ij}^t denote discrete azimuth AoA and AoD of jth ray in ith cluster, respectively.

$\mathbf{a}_\mathrm{r}(\theta_{ij}^\mathrm{r}) = \frac{1}{\sqrt{N_\mathrm{r}}}\left[1, e^{\mathrm{j}\pi\sin\theta_{ij}^\mathrm{r}}, \dots, e^{\mathrm{j}\pi(N_\mathrm{r}-1)\sin\theta_{ij}^\mathrm{r}}\right]^T \in \mathbb{C}^{N_\mathrm{r}\times 1}$ and $\mathbf{a}_\mathrm{t}(\theta_{ij}^\mathrm{t}) = \frac{1}{\sqrt{N_\mathrm{t}}}\left[1, e^{\mathrm{j}\pi\sin\theta_{ij}^\mathrm{t}}, \dots, e^{\mathrm{j}\pi(N_\mathrm{t}-1)\sin\theta_{ij}^\mathrm{t}}\right]^T \in \mathbb{C}^{N_\mathrm{t}\times 1}$ denote for normalized receive and transmit antenna array response vectors, respectively. Note that perfect CSI is assumed to be known in OFDM-JSC transmitter before hybrid beamforming design.

2.3 Radar Model

The transmit beampattern of OFDM-JSC transmitter is given as [18]

$$\mathrm{G}(\theta, k) = \mathbf{a}^H(\theta)\mathbf{R}[k]\mathbf{a}(\theta). \quad (4)$$

$\mathbf{a}(\theta)$ is transmit antenna array response vector as

$$\mathbf{a}(\theta) = \left[1, e^{\mathrm{j}\pi\sin\theta}, \dots, e^{\mathrm{j}\pi(N_\mathrm{t}-1)\sin\theta}\right]^T \in \mathbb{C}^{N_\mathrm{t}\times 1}. \quad (5)$$

Where θ denotes for discrete azimuth angle, and $-90° \le \theta \le 90°$. $\mathbf{R}[\mathrm{k}] \in \mathbb{C}^{N_\mathrm{t}\times N_\mathrm{t}}$ is the correlation matrix of baseband equivalent signal at kth subcarrier

$$\begin{aligned}\mathbf{R}[k] &= \mathbb{E}(\mathbf{F}_{\mathrm{RF}}\mathbf{F}_{\mathrm{BB}}[k]\mathbf{s}[k]\mathbf{s}^H[k]\mathbf{F}_{\mathrm{BB}}^H[k]\mathbf{F}_{\mathrm{RF}}^H) \\ &= \mathbf{F}_{\mathrm{RF}}\mathbf{F}_{\mathrm{BB}}[k]\mathbb{E}(\mathbf{s}[k]\mathbf{s}^H[k])\mathbf{F}_{\mathrm{BB}}^H[k]\mathbf{F}_{\mathrm{RF}}^H \\ &= \mathbf{F}_{\mathrm{RF}}\mathbf{F}_{\mathrm{BB}}[k]\mathbf{F}_{\mathrm{BB}}^H[k]\mathbf{F}_{\mathrm{RF}}^H. \end{aligned} \quad (6)$$

We can observe from (6) that designing the transmit beampattern is equivalent to designing the hybrid beamforming matrix.

Note that since we assume the carrier frequency of above OFDM-JSC system is much larger than its bandwidth [19], there is only a slight deviation between the antenna array response of lowest frequency subcarrier and highest frequency subcarrier [20]. Thus, we temporarily ignore the effect of subcarrier frequency in (5).

3 Problem Formulation

3.1 Communication Sub-problem

With optimal fully digital combiner in UE receiver, the spectral efficiency of OFDM-JSC system is given by [21]

$$SE = \frac{1}{K}\sum_{K=1}^{K} log_2 \left|\mathbf{I}_{N_\mathrm{s}} + \frac{\mathbf{W}^H[k]\mathbf{H}[k]\mathbf{F}_\mathrm{RF}\mathbf{F}_\mathrm{BB}[k]\mathbf{F}_\mathrm{BB}^H[k]\mathbf{F}_\mathrm{RF}^H\mathbf{H}^H[k]\mathbf{W}[k]}{\sigma_n^2}\right|. \quad (7)$$

To maximize the spectral efficiency of OFDM-JSC system, the hybrid beamforming matrix should be designed to approximate the optimal fully digital beamforming matrix $\mathbf{F}_\mathrm{com}[k] \in \mathbb{C}^{N_\mathrm{t}\times N_\mathrm{s}}$, which can be obtained via singular value decomposition (SVD) [22]

$$\mathbf{H}[k] = \mathbf{U}[k]\mathbf{\Sigma}[k]\mathbf{V}^H[k]. \quad (8)$$

$\mathbf{U}[k] = \left[\widetilde{\mathbf{U}}[k], \overline{\mathbf{U}}[k]\right] \in \mathbb{C}^{N_\mathrm{r}\times \mathrm{rank}(\mathbf{H}[k])}$ is the left singular value matrix of channel matrix $\mathbf{H}[k]$, where $\widetilde{\mathbf{U}}[k] \in \mathbb{C}^{N_\mathrm{r}\times N_\mathrm{s}}$. The optimal fully digital combining matrix for kth subcarrier in UE receiver is given by $\mathbf{W}[k] = \widetilde{\mathbf{U}}[k]$.

$\mathbf{V}[k] = \left[\widetilde{\mathbf{V}}[k], \overline{\mathbf{V}}[k]\right] \in \mathbb{C}^{N_\mathrm{t}\times \mathrm{rank}(\mathbf{H}[k])}$ is the right singular value matrix of channel matrix $\mathbf{H}[k]$, where $\widetilde{\mathbf{V}}[k] \in \mathbb{C}^{N_\mathrm{t}\times N_\mathrm{s}}$. The optimal fully digital beamforming matrix for kth subcarrier is given by $\mathbf{F}_\mathrm{com}[k] = \widetilde{\mathbf{V}}[k]$.

For HBF-OFDM-JSC transmitter, the sub-problem for downlink communication hybrid beamforming design can be modeled as [22]

$$\begin{aligned}\min_{\mathbf{F}_\mathrm{RF},\{\mathbf{F}_\mathrm{BB}[k]\}_{k\in\mathcal{K}}} \quad & \sum_{k\in\mathcal{K}}\|\mathbf{F}_\mathrm{RF}\mathbf{F}_\mathrm{BB}[k] - \mathbf{F}_\mathrm{com}[k]\|_F. \\ \text{s. t.} \quad & \sum_{k\in\mathcal{K}}\|\mathbf{F}_\mathrm{RF}\mathbf{F}_\mathrm{BB}[k]\|_F^2 = KP_T \\ & \left|[\mathbf{F}_\mathrm{RF}]_{i,j}\right| = 1, \forall i,j\end{aligned} \quad (9)$$

For HBP-OFDM-JSC transmitter, the constraints should be changed due to the special structure of $\mathbf{F}_\mathrm{RF}$. Thus, the corresponding sub-problem for downlink communication hybrid beamforming design can be modeled as

$$\begin{aligned}\min_{\mathbf{F}_\mathrm{RF},\{\mathbf{F}_\mathrm{BB}[k]\}_{k\in\mathcal{K}}} \quad & \sum_{k\in\mathcal{K}}\|\mathbf{F}_\mathrm{RF}\mathbf{F}_\mathrm{BB}[k] - \mathbf{F}_\mathrm{com}[k]\|_F. \\ \text{s. t.} \quad & \sum_{k\in\mathcal{K}}\|\mathbf{F}_\mathrm{BB}[k]\|_F^2 = \frac{KN_\mathrm{RF}P_T}{N_\mathrm{t}} \\ & \left|[\mathbf{F}_\mathrm{RF}]_{i,j}\right| = 1, \forall i,j \in \mathcal{L} \\ & \left|[\mathbf{F}_\mathrm{RF}]_{i,j}\right| = 0, \forall i,j \in \bar{\mathcal{L}}\end{aligned} \quad (10)$$

Where $\mathcal{L}$ denotes for the set of non-zero elements in $\mathbf{F}_\mathrm{RF}$ and $\bar{\mathcal{L}}$ denotes for the set of zero elements in $\mathbf{F}_\mathrm{RF}$, corresponds to (2).

3.2 Sensing Sub-problem

Suppose that there are N_tar directions of interest which need to be detected, the corresponding discrete azimuth angles are $\{\theta_1, \theta_2, \dots, \theta_{N_\mathrm{tar}}\}$. The baseline analog beamforming matrix for MIMO-OFDM radar is given by

$$\mathbf{F}_\mathrm{rad} = \left[\mathbf{a}(\theta_1), \mathbf{a}(\theta_2), \dots, \mathbf{a}\left(\theta_{N_\mathrm{tar}}\right)\right] \in \mathbb{C}^{N_\mathrm{t}\times N_\mathrm{tar}}. \quad (11)$$

$\mathbf{a}(\theta_i) = \left[1, e^{\mathrm{j}\pi\sin\theta_i}, \dots, e^{\mathrm{j}\pi(N_\mathrm{t}-1)\sin\theta_i}\right]^T \in \mathbb{C}^{N_\mathrm{t}\times 1}, i = 1, \dots, N_\mathrm{tar}$ is transmit antenna array response vector. While for the subarrayed MIMO-OFDM radar [23], the baseline analog beamforming matrix with a block diagonal structure is given by

$$\mathbf{F}_\mathrm{rad} = \begin{bmatrix}\mathbf{a}(\theta_1) & \mathbf{0} & \cdots & \mathbf{0} \\ \mathbf{0} & \mathbf{a}(\theta_2) & & \mathbf{0} \\ \vdots & & \ddots & \vdots \\ \mathbf{0} & \mathbf{0} & \cdots & \mathbf{a}\left(\theta_{N_\mathrm{tar}}\right)\end{bmatrix} \in \mathbb{C}^{N_\mathrm{t}\times N_\mathrm{tar}}. \quad (12)$$

$\mathbf{a}(\theta_i) = \left[1, e^{\mathrm{j}\pi\sin\theta_i}, \dots, e^{\mathrm{j}\pi\left(\frac{N_\mathrm{t}}{N_\mathrm{tar}}-1\right)\sin\theta_i}\right]^T \in \mathbb{C}^{\frac{N_\mathrm{t}}{N_\mathrm{tar}}\times 1}, i = 1, \dots, N_\mathrm{tar}$ is transmit antenna array response vector. The sub-problem for radar sensing hybrid beamforming design in OFDM-JSC transmitter can be modeled as

$$\begin{aligned}\min_{\mathbf{F}_\mathrm{RF},\{\mathbf{F}_\mathrm{BB}[k]\}_{k\in\mathcal{K}}} \quad & \sum_{k\in\mathcal{K}}\|\mathbf{F}_\mathrm{RF}\mathbf{F}_\mathrm{BB}[k] - \mathbf{F}_\mathrm{rad}\mathbf{A}[k]\|_F. \\ \text{s. t.} \quad & \mathbf{A}[k]\mathbf{A}^H[k] = \mathbf{I}_{N_\mathrm{tar}}\end{aligned} \quad (13)$$

Where $\mathbf{A}[k] \in \mathbb{C}^{N_\mathrm{tar}\times N_\mathrm{s}}, k = 1, \dots, K$ is the auxiliary unitary matrix which can match the dimensions of $\mathbf{F}_\mathrm{RF}\mathbf{F}_\mathrm{BB}[k] \in \mathbb{C}^{N_\mathrm{t}\times N_\mathrm{s}}$ and $\mathbf{F}_\mathrm{rad} \in \mathbb{C}^{N_\mathrm{t}\times N_\mathrm{tar}}$ without changing the desired transmit beampattern.

3.3 Joint Optimization Problem

To solve the sub-problems for downlink communication and radar sensing above, we formulate the JSC beamforming design as a weighted minimization problem where the optimal fully digital beamforming matrix and the baseline radar beamforming matrix are respectively approached depending on the weights assigned to downlink communication and radar sensing. For HBF-OFDM-JSC transmitter, we construct the beamforming problem as

$$\begin{aligned}\min_{\mathbf{F}_\mathrm{RF},\{\mathbf{F}_\mathrm{BB}[k],\mathbf{A}[k]\}_{k\in\mathcal{K}}} \quad & \sum_{k\in\mathcal{K}}\{\eta\|\mathbf{F}_\mathrm{RF}\mathbf{F}_\mathrm{BB}[k] - \mathbf{F}_\mathrm{com}[k]\|_F + \\ & (1-\eta)\|\mathbf{F}_\mathrm{RF}\mathbf{F}_\mathrm{BB}[k] - \mathbf{F}_\mathrm{rad}\mathbf{A}[k]\|_F\} \\ \text{s. t.} \quad & \sum_{k\in\mathcal{K}}\|\mathbf{F}_\mathrm{RF}\mathbf{F}_\mathrm{BB}[k]\|_F^2 = KP_T \\ & \left|[\mathbf{F}_\mathrm{RF}]_{i,j}\right| = 1, \forall i,j \\ & \mathbf{A}[k]\mathbf{A}^H[k] = \mathbf{I}_{N_\mathrm{tar}}.\end{aligned} \quad (14)$$

Correspondingly, for HBP-OFDM-JSC transmitter, we construct the beamforming problem as

$$\begin{aligned}\min_{\mathbf{F}_\mathrm{RF},\{\mathbf{F}_\mathrm{BB}[k],\mathbf{A}[k]\}_{k\in\mathcal{K}}} \quad & \sum_{k\in\mathcal{K}}\{\eta\|\mathbf{F}_\mathrm{RF}\mathbf{F}_\mathrm{BB}[k] - \mathbf{F}_\mathrm{com}[k]\|_F + \\ & (1-\eta)\|\mathbf{F}_\mathrm{RF}\mathbf{F}_\mathrm{BB}[k] - \mathbf{F}_\mathrm{rad}\mathbf{A}[k]\|_F\} \\ \text{s. t.} \quad & \sum_{k\in\mathcal{K}}\|\mathbf{F}_\mathrm{BB}[k]\|_F^2 = \frac{KN_\mathrm{RF}P_T}{N_\mathrm{t}} \\ & \left|[\mathbf{F}_\mathrm{RF}]_{i,j}\right| = 1, \forall i,j \in \mathcal{L} \\ & \left|[\mathbf{F}_\mathrm{RF}]_{i,j}\right| = 0, \forall i,j \in \bar{\mathcal{L}}\end{aligned}$$

$$\mathbf{A}[k]\mathbf{A}^H[k] = \mathbf{I}_{N_{\mathrm{tar}}}. \quad (15)$$

$\eta \in [0,1]$ is an artificially set weighting factor, which can provide a trade-off between downlink communication and radar sensing for OFDM-JSC system. If $\eta = 1$ ($\eta = 0$), (14) or (15) is equal to a communication-only (sensing-only) hybrid beamforming problem.

4 Alternating Optimization

We propose low-complexity alternating optimization methods in the following that can provide near-optimal solutions to problem (14) and (15), through which $\mathbf{F}_{\mathrm{RF}}$, $\{\mathbf{F}_{\mathrm{BB}}[k]\}_{k\in\mathcal{K}}$, as well as $\{\mathbf{A}[k]\}_{k\in\mathcal{K}}$ are estimated one-by-one while the others are fixed.

4.1 Alternating Optimization Algorithm for HBP-JSC Transmitter

By fixing $\mathbf{F}_{\mathrm{RF}}$ and $\{\mathbf{F}_{\mathrm{BB}}[k]\}_{k\in\mathcal{K}}$, we first optimize $\{\mathbf{A}[k]\}_{k\in\mathcal{K}}$ by solving the following problem

$$\begin{aligned}\min_{\{\mathbf{A}[k]\}_{k\in\mathcal{K}}} \ & \textstyle\sum_{k\in\mathcal{K}} \|\mathbf{F}_{\mathrm{rad}}\mathbf{A}[k] - \mathbf{F}_{\mathrm{RF}}\mathbf{F}_{\mathrm{BB}}[k]\|_F^2 \\ \text{s.t.} \ & \mathbf{A}[k]\mathbf{A}^H[k] = \mathbf{I}_{N_{\mathrm{tar}}}. \end{aligned} \quad (16)$$

Note that (16) is equivalent to an Orthogonal Procrustes problem (OPP). And we can optimally solve (16) via singular value decomposition (SVD) [24]

$$\mathbf{F}_{\mathrm{rad}}^H\mathbf{F}_{\mathrm{RF}}\mathbf{F}_{\mathrm{BB}}[k] = \mathbf{U}[k]\mathbf{\Sigma}[k]\mathbf{V}^H[k]. \quad (17)$$

Then the globally optimal solution of $\{\mathbf{A}[k]\}_{k\in\mathcal{K}}$ is given by

$$\mathbf{A}[k] = \mathbf{U}[k]\mathbf{I}_{N_{\mathrm{tar}}\times N_{\mathrm{s}}}\mathbf{V}^H[k]. \quad (18)$$

According to the triangle inequality of norm, we have

$$\begin{aligned} & \eta\|\mathbf{F}_{\mathrm{RF}}\mathbf{F}_{\mathrm{BB}}[k] - \mathbf{F}_{\mathrm{com}}[k]\|_F + (1-\eta)\|\mathbf{F}_{\mathrm{RF}}\mathbf{F}_{\mathrm{BB}}[k] - \mathbf{F}_{\mathrm{rad}}\mathbf{A}[k]\|_F \\ & \geq \|\eta(\mathbf{F}_{\mathrm{RF}}\mathbf{F}_{\mathrm{BB}}[k] - \mathbf{F}_{\mathrm{com}}[k]) + (1-\eta)(\mathbf{F}_{\mathrm{RF}}\mathbf{F}_{\mathrm{BB}}[k] - \mathbf{F}_{\mathrm{rad}}\mathbf{A}[k])\|_F \\ & = \|\mathbf{F}_{\mathrm{RF}}\mathbf{F}_{\mathrm{BB}}[k] - \eta\mathbf{F}_{\mathrm{com}}[k] - (1-\eta)\mathbf{F}_{\mathrm{rad}}\mathbf{A}[k]\|_F. \end{aligned} \quad (19)$$

Then we can rewrite the objective function of (14) and (15) as

$$\textstyle\sum_{k\in\mathcal{K}} \|\mathbf{F}_{\mathrm{RF}}\mathbf{F}_{\mathrm{BB}}[k] - \mathbf{F}_{\mathrm{CR}}[k]\|_F^2. \quad (20)$$

Where $\mathbf{F}_{\mathrm{CR}}[k] = \eta\mathbf{F}_{\mathrm{com}}[k] + (1-\eta)\mathbf{F}_{\mathrm{rad}}\mathbf{A}[k] \in \mathbb{C}^{N_{\mathrm{t}}\times N_{\mathrm{s}}}$. Note that when we fix $\{\mathbf{A}[k]\}_{k\in\mathcal{K}}$, the matrix $\{\mathbf{F}_{\mathrm{CR}}[k]\}_{k\in\mathcal{K}}$ is also fixed. Then we substitute (20) into (15), and fix $\mathbf{F}_{\mathrm{RF}}$ and $\{\mathbf{A}[k]\}_{k\in\mathcal{K}}$, the optimization for $\{\mathbf{F}_{\mathrm{BB}}[k]\}_{k\in\mathcal{K}}$ can be written as

$$\begin{aligned}\min_{\{\mathbf{F}_{\mathrm{BB}}[k]\}_{k\in\mathcal{K}}} \ & \textstyle\sum_{k\in\mathcal{K}} \|\mathbf{F}_{\mathrm{RF}}\mathbf{F}_{\mathrm{BB}}[k] - \mathbf{F}_{\mathrm{CR}}[k]\|_F^2. \\ \text{s.t.} \ & \textstyle\sum_{k\in\mathcal{K}} \|\mathbf{F}_{\mathrm{BB}}[k]\|_F^2 = \frac{KN_{\mathrm{RF}}P_T}{N_{\mathrm{t}}} \end{aligned} \quad (21)$$

The least squares solution of $\{\mathbf{F}_{\mathrm{BB}}[k]\}_{k\in\mathcal{K}}$ in (21) is given by

$$\mathbf{F}_{\mathrm{BB}}[k] = \mathbf{F}_{\mathrm{RF}}^{\dagger}\mathbf{F}_{\mathrm{CR}}[k]. \quad (22)$$

Now we fix $\{\mathbf{F}_{\mathrm{BB}}[k]\}_{k\in\mathcal{K}}$ and $\{\mathbf{A}[k]\}_{k\in\mathcal{K}}$, as well as $\{\mathbf{F}_{\mathrm{CR}}[k]\}_{k\in\mathcal{K}}$, and rewrite the optimization problem for $\mathbf{F}_{\mathrm{RF}}$ in a more compact form as

$$\begin{aligned}\min_{\mathbf{F}_{\mathrm{RF}}} \ & \left\|\mathbf{F}_{\mathrm{RF}}\tilde{\mathbf{F}}_{\mathrm{BB}} - \tilde{\mathbf{F}}_{\mathrm{CR}}\right\|_F^2. \\ \text{s.t.} \ & \left|[\mathbf{F}_{\mathrm{RF}}]_{i,j}\right| = 1, \forall i,j \in \mathcal{L} \\ & \left|[\mathbf{F}_{\mathrm{RF}}]_{i,j}\right| = 0, \forall i,j \in \bar{\mathcal{L}} \end{aligned} \quad (23)$$

As we define

$\tilde{\mathbf{F}}_{\mathrm{BB}} = \left[\mathbf{F}_{\mathrm{BB}}[1], \mathbf{F}_{\mathrm{BB}}[2], \cdots, \mathbf{F}_{\mathrm{BB}}[K]\right] \in \mathbb{C}^{N_{\mathrm{RF}}\times KN_{\mathrm{s}}}$,

$\tilde{\mathbf{F}}_{\mathrm{CR}} = \eta\tilde{\mathbf{F}}_{\mathrm{com}} + (1-\eta)\mathbf{F}_{\mathrm{rad}}\tilde{\mathbf{A}}$

$= \left[\mathbf{F}_{\mathrm{CR}}[1], \mathbf{F}_{\mathrm{CR}}[2], \cdots, \mathbf{F}_{\mathrm{CR}}[K]\right] \in \mathbb{C}^{N_{\mathrm{t}}\times KN_{\mathrm{s}}}$,

$\tilde{\mathbf{A}} = \left[\mathbf{A}[1], \cdots, \mathbf{A}[K]\right] \in \mathbb{C}^{N_{\mathrm{tar}}\times KN_{\mathrm{s}}}$,

$\tilde{\mathbf{F}}_{\mathrm{com}} = \left[\mathbf{F}_{\mathrm{com}}[1], \cdots, \mathbf{F}_{\mathrm{com}}[K]\right] \in \mathbb{C}^{N_{\mathrm{t}}\times KN_{\mathrm{s}}}$.

Due to the special structure of $\mathbf{F}_{\mathrm{RF}}$ as (2), the near-optimal solution of (23) can be obtained via phase rotation

$$(\mathbf{F}_{\mathrm{RF}})_{i,j} = \exp\left(1\mathrm{j} * \arg\left[\left(\tilde{\mathbf{F}}_{\mathrm{CR}}\right)_{i,:}\left(\tilde{\mathbf{F}}_{\mathrm{BB}}\right)_{j,:}^H\right]\right), \forall i,j \in \mathcal{L}. \quad (24)$$

Where 1j stands for the imaginary unit. Lastly, in order to guarantee the transmit power constraint in (15), we should normalize the digital beamforming matrix as $\mathbf{F}_{\mathrm{BB}}[k] = \sqrt{\frac{P_T N_{\mathrm{RF}}}{N_{\mathrm{t}}}}\frac{\mathbf{F}_{\mathrm{BB}}[k]}{\|\mathbf{F}_{\mathrm{BB}}[k]\|_F}, k \in \mathcal{K} = \{1, \ldots, K\}$. The alternating optimization algorithm for HBP-JSC beamforming is summarized in Algorithm 1.

Algorithm 1. Alternating optimization algorithm to solve (15)

Input: $\mathbf{H}[k] \in \mathbb{C}^{N_{\mathrm{r}}\times N_{\mathrm{t}}}$, $\mathbf{F}_{\mathrm{com}}[k] \in \mathbb{C}^{N_{\mathrm{t}}\times N_{\mathrm{s}}}$, $\mathbf{F}_{\mathrm{rad}} \in \mathbb{C}^{N_{\mathrm{t}}\times N_{\mathrm{tar}}}$, $\eta \in [0,1]$, P_T, $k \in \mathcal{K} = \{1, \ldots, K\}$

Output: $\mathbf{F}_{\mathrm{RF}} \in \mathbb{C}^{N_{\mathrm{t}}\times N_{\mathrm{RF}}}$, $\mathbf{F}_{\mathrm{BB}}[k] \in \mathbb{C}^{N_{\mathrm{RF}}\times N_{\mathrm{s}}}, k \in \mathcal{K} = \{1, \ldots, K\}$

1: Initialize $\mathbf{F}_{\mathrm{RF}} \in \mathbb{C}^{N_{\mathrm{t}}\times N_{\mathrm{RF}}}$, $\mathbf{F}_{\mathrm{BB}}[k] \in \mathbb{C}^{N_{\mathrm{RF}}\times N_{\mathrm{s}}}, k \in \mathcal{K} = \{1, \ldots, K\}$.

2: **repeat**

3: Compute $\mathbf{A}[k] \in \mathbb{C}^{N_{\mathrm{tar}}\times N_{\mathrm{s}}}, k \in \mathcal{K} = \{1, \ldots, K\}$ by (18), and construct $\mathbf{F}_{\mathrm{CR}}[k] = \eta\mathbf{F}_{\mathrm{com}}[k] + (1-\eta)\mathbf{F}_{\mathrm{rad}}\mathbf{A}[k] \in \mathbb{C}^{N_{\mathrm{t}}\times N_{\mathrm{s}}}, k \in \mathcal{K} = \{1, \ldots, K\}$.

4: Compute $\mathbf{F}_{\mathrm{BB}}[k] \in \mathbb{C}^{N_{\mathrm{RF}}\times N_{\mathrm{s}}}, k \in \mathcal{K} = \{1, \ldots, K\}$ by (22), and construct $\tilde{\mathbf{F}}_{\mathrm{BB}} \in \mathbb{C}^{N_{\mathrm{RF}}\times KN_{\mathrm{s}}}$, $\tilde{\mathbf{F}}_{\mathrm{CR}} \in \mathbb{C}^{N_{\mathrm{t}}\times KN_{\mathrm{s}}}$.

5: Compute $\mathbf{F}_{\mathrm{RF}} \in \mathbb{C}^{N_{\mathrm{t}}\times N_{\mathrm{RF}}}$ by (24).

6: **until** convergence

7: Normalize $\mathbf{F}_{\mathrm{BB}}[k] = \sqrt{\frac{P_T N_{\mathrm{RF}}}{N_{\mathrm{t}}}}\frac{\mathbf{F}_{\mathrm{BB}}[k]}{\|\mathbf{F}_{\mathrm{BB}}[k]\|_F}, k \in \mathcal{K} = \{1, \ldots, K\}$.

4.2 Alternating Optimization Algorithm for HBF-JSC Transmitter

Now we discuss the alternating optimization to solve (14). Similar to Algorithm 1, we first fix $\mathbf{F}_{\mathrm{RF}}$ and $\{\mathbf{F}_{\mathrm{BB}}[k]\}_{k\in\mathcal{K}}$, then the globally optimal solution for $\{\mathbf{A}[k]\}_{k\in\mathcal{K}}$ can also be obtained via (18). Then we fix $\{\mathbf{A}[k]\}_{k\in\mathcal{K}}$ as well as $\{\mathbf{F}_{\mathrm{CR}}[k]\}_{k\in\mathcal{K}}$, the alternating optimization for $\mathbf{F}_{\mathrm{RF}}$ and $\{\mathbf{F}_{\mathrm{BB}}[k]\}_{k\in\mathcal{K}}$ in HBF-JSC transmitter can be modeled as

$$\min_{\mathbf{F}_{\mathrm{RF}},\{\mathbf{F}_{\mathrm{BB}}[k]\}_{k\in\mathcal{K}}} \sum_{k\in\mathcal{K}}\|\mathbf{F}_{\mathrm{CR}}[k]-\mathbf{F}_{\mathrm{RF}}\mathbf{F}_{\mathrm{BB}}[k]\|_F^2. \quad \text{s.t.} \quad \sum_{k\in\mathcal{K}}\|\mathbf{F}_{\mathrm{RF}}\mathbf{F}_{\mathrm{BB}}[k]\|_F^2 = KP_T \quad \left|[\mathbf{F}_{\mathrm{RF}}]_{i,j}\right| = 1, \forall i,j \tag{25}$$

Note that (25) is similar to the communication-only hybrid beamforming problem in (9). Here we recommend PE-AltMin Algorithm [25] to estimated $\mathbf{F}_{\mathrm{RF}}$ and $\{\mathbf{F}_{\mathrm{BB}}[k]\}_{k\in\mathcal{K}}$ when $\{\mathbf{A}[k]\}_{k\in\mathcal{K}}$ is fixed. We first fix $\mathbf{F}_{\mathrm{RF}}$ and $\{\mathbf{A}[k]\}_{k\in\mathcal{K}}$, as well as $\{\mathbf{F}_{\mathrm{CR}}[k]\}_{k\in\mathcal{K}}$, and temporarily ignore the transmit power constraint, then the unconstrained digital beamforming matrix $\{\mathbf{F}_{\mathrm{DD}}[k]\}_{k\in\mathcal{K}}$ can be obtained via singular value decomposition (SVD)

$$\mathbf{F}_{\mathrm{CR}}^H[k]\mathbf{F}_{\mathrm{RF}} = \mathbf{U}[k]\mathbf{\Sigma}[k]\mathbf{V}^H[k]. \tag{26}$$

Then the globally optimal solution can be obtained by

$$\mathbf{F}_{\mathrm{DD}}[k] = \mathbf{V}[k]\mathbf{I}_{N_{\mathrm{RF}}\times N_{\mathrm{s}}}\mathbf{U}^H[k]. \tag{27}$$

After all the $\{\mathbf{F}_{\mathrm{DD}}[k]\}_{k\in\mathcal{K}}$ have been updated in parallel, we can get the closed-form solution of $\mathbf{F}_{\mathrm{RF}}$ through

$$\arg(\mathbf{F}_{\mathrm{RF}}) = \arg\left(\sum_{k=1}^{K}\mathbf{F}_{\mathrm{CR}}[k]\mathbf{F}_{\mathrm{DD}}^H[k]\right). \tag{28}$$

Finally, in order to guarantee the transmit power constraint in (14), we should normalize the digital beamforming matrix as $\mathbf{F}_{\mathrm{BB}}[k] = \frac{\sqrt{P_T}}{\|\mathbf{F}_{\mathrm{RF}}\mathbf{F}_{\mathrm{BB}}[k]\|_F}\mathbf{F}_{\mathrm{DD}}[k], k\in\mathcal{K}=\{1,\dots,K\}$. The alternating optimization algorithm for HBF-JSC beamforming is summarized in Algorithm 2.

Algorithm 2. Alternating optimization algorithm to solve (14)

Input: $\mathbf{H}[k]\in\mathbb{C}^{N_{\mathrm{r}}\times N_{\mathrm{t}}}$, $\mathbf{F}_{\mathrm{com}}[k]\in\mathbb{C}^{N_{\mathrm{t}}\times N_{\mathrm{s}}}$, $\mathbf{F}_{\mathrm{rad}}\in\mathbb{C}^{N_{\mathrm{t}}\times N_{\mathrm{tar}}}$, $\eta\in[0,1]$, P_T, $k\in\mathcal{K}=\{1,\dots,K\}$

Output: $\mathbf{F}_{\mathrm{RF}}\in\mathbb{C}^{N_{\mathrm{t}}\times N_{\mathrm{RF}}}$, $\mathbf{F}_{\mathrm{BB}}[k]\in\mathbb{C}^{N_{\mathrm{RF}}\times N_{\mathrm{s}}}, k\in\mathcal{K}=\{1,\dots,K\}$

1: Initialize $\mathbf{F}_{\mathrm{RF}}\in\mathbb{C}^{N_{\mathrm{t}}\times N_{\mathrm{RF}}}$, $\mathbf{F}_{\mathrm{BB}}[k]\in\mathbb{C}^{N_{\mathrm{RF}}\times N_{\mathrm{s}}}, k\in\mathcal{K}=\{1,\dots,K\}$.

2: **repeat**

3: Compute $\mathbf{A}[k]\in\mathbb{C}^{N_{\mathrm{tar}}\times N_{\mathrm{s}}}, k\in\mathcal{K}=\{1,\dots,K\}$ by (18), and construct $\mathbf{F}_{\mathrm{CR}}[k]=\eta\mathbf{F}_{\mathrm{com}}[k]+(1-\eta)\mathbf{F}_{\mathrm{rad}}\mathbf{A}[k]\in\mathbb{C}^{N_{\mathrm{t}}\times N_{\mathrm{s}}}, k\in\mathcal{K}=\{1,\dots,K\}$.

4: Compute $\mathbf{F}_{\mathrm{DD}}[k]\in\mathbb{C}^{N_{\mathrm{RF}}\times N_{\mathrm{s}}}, k\in\mathcal{K}=\{1,\dots,K\}$ by (27).

5: Compute $\mathbf{F}_{\mathrm{RF}}\in\mathbb{C}^{N_{\mathrm{t}}\times N_{\mathrm{RF}}}$ by (28).

6: **until** convergence

7: Normalize $\mathbf{F}_{\mathrm{BB}}[k]=\frac{\sqrt{P_T}}{\|\mathbf{F}_{\mathrm{RF}}\mathbf{F}_{\mathrm{BB}}[k]\|_F}\mathbf{F}_{\mathrm{DD}}[k], k\in\mathcal{K}=\{1,\dots,K\}$.

5 Beamforming Design for MU-MISO JSC

5.1 System Model

Now we consider an OFDM-JSC system serving N_{U} single receive antenna UEs, while steering probe beams towards N_{tar} directions. It is worth noting that $N_{\mathrm{U}}\le N_{\mathrm{t}}$ must be satisfied. And different from SU-MIMO scenario, the digital beamforming structure with N_{t} antennas ULA is equipped in JSC transmitter in multi-user MISO (MU-MISO) scenario, as shown in Figure 2.

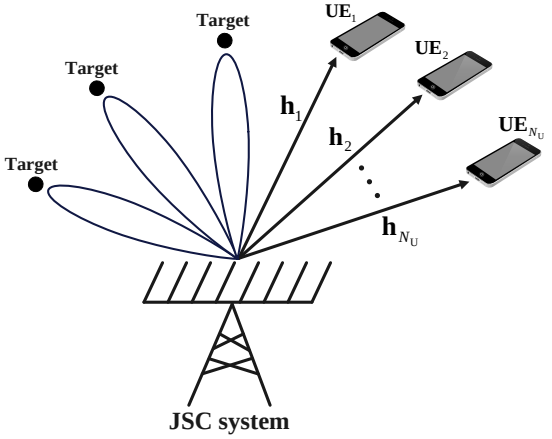

Figure 2. JSC beamforming in MU-MISO scenario

After the baseband demodulation operation in uth UE, the received symbol at kth subcarrier can be expressed as

$$\mathrm{y}_u[k] = \mathbf{h}_u[k]\mathbf{F}[k]\mathbf{s}[k] + \mathrm{n}_u[k]. \tag{29}$$

$\mathbf{s}[k]=\left[\mathrm{s}_1[k],\dots,\mathrm{s}_{N_{\mathrm{U}}}[k]\right]^T\in\mathbb{C}^{N_{\mathrm{U}}\times 1}, k\in\mathcal{K}=\{1,\dots,K\}$ denotes for the symbol vector transmitted towards N_{U} UEs at k th subcarrier, which satisfies that $\mathbb{E}\{\mathbf{s}[k]\mathbf{s}^H[k]\}=\mathbf{I}_{N_{\mathrm{U}}}$. K is the total number of subcarriers.

$\mathbf{h}_u[k]\in\mathbb{C}^{1\times N_{\mathrm{t}}}, u=1,\dots,N_{\mathrm{U}}$ denotes for the frequency domain channel vector at kth subcarrier between JSC system and uth UE. Then we can rewrite (29) into a more compact form as

$$\mathbf{y}[k] = \mathbf{H}[k]\mathbf{F}[k]\mathbf{s}[k] + \mathbf{n}[k]. \tag{30}$$

$\mathbf{H}[k]=\left[\mathbf{h}_1[k];\mathbf{h}_2[k];\dots;\mathbf{h}_{N_{\mathrm{U}}}[k]\right]\in\mathbb{C}^{N_{\mathrm{U}}\times N_{\mathrm{t}}}$ is the frequency domain channel matrix at kth subcarrier and $\mathbf{n}[k]\in\mathbb{C}^{N_{\mathrm{U}}\times 1}$ represents the complex AWGN vector at kth subcarrier, whose elements obey independent and identical distribution $\mathcal{CN}(0,\sigma_n^2)$.

Note that digital beamforming matrix $\mathbf{F}[k]\in\mathbb{C}^{N_{\mathrm{t}}\times N_{\mathrm{U}}}$ is performed for each subcarrier. Let P_T denotes the average transmit power per subcarrier, for the whole bandwidth we have the constraint $\sum_{k\in\mathcal{K}}\|\mathbf{F}[k]\|_F^2 = KP_T$.

The correlation matrix of baseband equivalent signal at kth subcarrier can be expressed as

$$\begin{aligned}\mathbf{R}[k] &= \mathbb{E}(\mathbf{F}[k]\mathbf{s}[k]\mathbf{s}^H[k]\mathbf{F}^H[k]) \\ &= \mathbf{F}[k]\mathbb{E}(\mathbf{s}[k]\mathbf{s}^H[k])\mathbf{F}^H[k] = \mathbf{F}[k]\mathbf{F}^H[k].\end{aligned} \tag{31}$$

The beampattern of JSC transmitter can also be obtained through (4). We can observe from (31) that designing transmit beampattern is equivalent to designing beamforming matrix. Note that (30) can be rewritten as

$$\begin{aligned}\mathbf{y}[k] &= \mathbf{s}[k] + (\mathbf{H}[k]\mathbf{F}[k]\mathbf{s}[k] - \mathbf{s}[k]) + \mathbf{n}[k] \\ &= \mathbf{s}[k] + \left(\mathbf{H}[k]\mathbf{F}[k] - \mathbf{I}_{N_{\mathrm{U}}}\right)\mathbf{s}[k] + \mathbf{n}[k].\end{aligned} \tag{32}$$

Notice that the second term above can be viewed as multiuser interference. And the total power of multiuser interference at k th subcarrier can be measured as $\left\|\mathbf{H}[k]\mathbf{F}[k]-\mathbf{I}_{N_\mathrm{U}}\right\|_F^2$. The SINR for uth UE is [26]

$$\mathrm{SINR}_u[k]=\frac{\mathbb{E}(|\mathrm{s}_u[k]|^2)}{\mathbb{E}(|\mathbf{h}_u[k]\mathbf{F}[k]\mathbf{s}[k]-\mathrm{s}_u[k]|^2)+\sigma_n^2}\ . \tag{33}$$

Then the spectral efficiency of JSC system is given by

$$\mathrm{SE}=\frac{1}{K}\sum_{k=1}^{K}\sum_{u=1}^{N_\mathrm{U}}\log_2(1+\mathrm{SINR}_u[k]). \tag{34}$$

For the sake of simplicity, we only use narrowband OFDM as an example and omit the subcarrier index k in the following. The channel vector between JSC system and uth UE can be modeled as [27]

$$\mathbf{h}_u=\sqrt{\frac{N_\mathrm{t}}{N_\mathrm{C}}}\sum_{i=1}^{N_\mathrm{C}}\alpha_i^u\mathbf{a}^H(\theta_i^u),u=1,\dots,N_\mathrm{U}. \tag{35}$$

Assuming the same number of propagation paths from JSC transmitter to each UE, denoted by N_C. α_i^u is the complex gain of ith path to uth UE following complex Gaussian distribution $\alpha_i^u\sim\mathcal{CN}(0,1)$. θ_i^u is discrete azimuth AoD of ith path to uth UE.

$\mathbf{a}(\theta_i^u)=\frac{1}{\sqrt{N_\mathrm{t}}}\left[1,e^{\mathrm{j}\pi\sin\theta_i^u},\dots,e^{\mathrm{j}\pi(N_\mathrm{t}-1)\sin\theta_i^u}\right]^T\in$ $\mathbb{C}^{N_\mathrm{t}\times1}$ denotes for normalized transmit antenna array response vector. Note that the number of UEs and perfect CSI are assumed to be known in JSC transmitter before beamforming design.

5.2 JSC Beamforming Design with Sensing-and-Communication Trade-off

Similar to (14) and (15), we provide JSC system with a trade-off between radar sensing and downlink communication by artificially defining the weight factor $\eta\in[0,1]$. We first impose transmit power constraint over total antenna array, then we construct the weighted minimization problem for JSC beamforming as

$$\begin{aligned}&\min_{\mathbf{F}}\ \eta\left\|\mathbf{HF}-\mathbf{I}_{N_\mathrm{U}}\right\|_F^2+(1-\eta)\|\mathbf{F}-\mathbf{F}_0\|_F^2.\\&\text{s.t. }\|\mathbf{F}\|_F^2=P_T\end{aligned} \tag{36}$$

Where $\mathbf{F}_0\in\mathbb{C}^{N_\mathrm{t}\times N_\mathrm{U}}$ is the digital beamforming matrix corresponding to the baseline radar beampattern, which can be constructed by

$$\mathbf{F}_0=\left[\mathbf{F}_\mathrm{rad},\mathbf{0}_{N_\mathrm{t}\times(N_\mathrm{U}-N_\mathrm{tar})}\right]\in\mathbb{C}^{N_\mathrm{t}\times N_\mathrm{U}}. \tag{37}$$

$\mathbf{F}_\mathrm{rad}\in\mathbb{C}^{N_\mathrm{t}\times N_\mathrm{tar}}$ is the analog beamforming matrix corresponding to the baseline radar beampattern, which can be constructed by the method similar to (11)

$$\mathbf{F}_\mathrm{rad}=\left[\mathbf{a}(\theta_1),\mathbf{a}(\theta_2),\dots,\mathbf{a}\left(\theta_{N_\mathrm{tar}}\right)\right]\in\mathbb{C}^{N_\mathrm{t}\times N_\mathrm{tar}}. \tag{38}$$

Now we rewrite the objective function of (36) as

$$\begin{aligned}&\eta\left\|\mathbf{HF}-\mathbf{I}_{N_\mathrm{U}}\right\|_F^2+(1-\eta)\|\mathbf{F}-\mathbf{F}_0\|_F^2.\\&=\left\|\left[\sqrt{\eta}\mathbf{H};\sqrt{1-\eta}\mathbf{I}_{N_\mathrm{t}}\right]\mathbf{F}-\left[\sqrt{\eta}\mathbf{I}_{N_\mathrm{U}};\sqrt{1-\eta}\mathbf{F}_0\right]\right\|_F^2\end{aligned} \tag{39}$$

Then we define
$\mathbf{A}=\left[\sqrt{\eta}\mathbf{H};\sqrt{1-\eta}\mathbf{I}_{N_\mathrm{t}}\right]\in\mathbb{C}^{(N_\mathrm{U}+N_\mathrm{t})\times N_\mathrm{t}}$,
$\mathbf{B}=\left[\sqrt{\eta}\mathbf{I}_{N_\mathrm{U}};\sqrt{1-\eta}\mathbf{F}_0\right]\in\mathbb{C}^{(N_\mathrm{U}+N_\mathrm{t})\times N_\mathrm{U}}$.
The objective function of (36) can be rewritten as

$$\begin{aligned}&\|\mathbf{AF}-\mathbf{B}\|_F^2=\mathrm{tr}[(\mathbf{AF}-\mathbf{B})(\mathbf{AF}-\mathbf{B})^H]\\&=\mathrm{tr}(\mathbf{F}^H\mathbf{A}^H\mathbf{AF})-\mathrm{tr}(\mathbf{F}^H\mathbf{A}^H\mathbf{B})-\mathrm{tr}(\mathbf{B}^H\mathbf{AF}).\end{aligned} \tag{40}$$

By defining $\boldsymbol{\mathcal{A}}=\mathbf{A}^H\mathbf{A}$, $\boldsymbol{\mathcal{B}}=\mathbf{A}^H\mathbf{B}$, and substituting (40) into (36), we have

$$\begin{aligned}&\min_{\mathbf{F}}\ \mathrm{tr}(\mathbf{F}^H\boldsymbol{\mathcal{A}}\mathbf{F})-\mathrm{tr}(\mathbf{F}^H\boldsymbol{\mathcal{B}})-\mathrm{tr}(\boldsymbol{\mathcal{B}}^H\mathbf{F}).\\&\text{s.t. }\|\mathbf{F}\|_F^2=P_T\end{aligned} \tag{41}$$

Then the Lagrange Multiplier method is used to solve (41). The Lagrangian function is defined as

$$\begin{aligned}L(\mathbf{F},\lambda)=&\ \mathrm{tr}(\mathbf{F}^H\boldsymbol{\mathcal{A}}\mathbf{F})-\mathrm{tr}(\mathbf{F}^H\boldsymbol{\mathcal{B}})\\&-\mathrm{tr}(\boldsymbol{\mathcal{B}}^H\mathbf{F})+\lambda(\|\mathbf{F}\|_F^2-P_T).\end{aligned} \tag{42}$$

λ is the Lagrange Multiplier. Then we take the derivative of Lagrangian function (42) as

$$\nabla L(\mathbf{F},\lambda)=2\left(\boldsymbol{\mathcal{A}}+\lambda\mathbf{I}_{N_\mathrm{t}}\right)\mathbf{F}-2\boldsymbol{\mathcal{B}}. \tag{43}$$

Then we can obtain the optimal digital beamforming matrix $\mathbf{F}_\mathrm{opt}$ by setting (43) equal to zero

$$2\left(\boldsymbol{\mathcal{A}}+\lambda_\mathrm{opt}\mathbf{I}_{N_\mathrm{t}}\right)\mathbf{F}_\mathrm{opt}-2\boldsymbol{\mathcal{B}}=\mathbf{0}. \tag{44}$$

$$\mathbf{F}_\mathrm{opt}=\left(\boldsymbol{\mathcal{A}}+\lambda_\mathrm{opt}\mathbf{I}_{N_\mathrm{t}}\right)^\dagger\boldsymbol{\mathcal{B}}. \tag{45}$$

The second derivative of Lagrangian function (42) is $\left(\boldsymbol{\mathcal{A}}+\lambda\mathbf{I}_{N_\mathrm{t}}\right)$. To ensure the existence of minimum point, the second derivative of Lagrangian function, also known as Hessian matrix, must be positive definite, which means that all eigenvalues of matrix $\left(\boldsymbol{\mathcal{A}}+\lambda_\mathrm{opt}\mathbf{I}_{N_\mathrm{t}}\right)$ must be greater than 0. The eigenvalue decomposition (EVD) of matrix $\left(\boldsymbol{\mathcal{A}}+\lambda_\mathrm{opt}\mathbf{I}_{N_\mathrm{t}}\right)$ is given by

$$\left(\boldsymbol{\mathcal{A}}+\lambda_\mathrm{opt}\mathbf{I}_{N_\mathrm{t}}\right)=\mathbf{V}\left(\boldsymbol{\Sigma}+\lambda_\mathrm{opt}\mathbf{I}_{N_\mathrm{t}}\right)\mathbf{V}^{-1}. \tag{46}$$

Where $\boldsymbol{\mathcal{A}}=\mathbf{V}\boldsymbol{\Sigma}\mathbf{V}^{-1}$ is the eigenvalue decomposition (EVD) of matrix $\boldsymbol{\mathcal{A}}$, $\mathbf{V}\in\mathbb{C}^{N_\mathrm{t}\times N_\mathrm{t}}$ is a unitary matrix which contains the eigenvectors of matrix $\boldsymbol{\mathcal{A}}$, and satisfies $\mathbf{V}^{-1}=\mathbf{V}^H$. $\boldsymbol{\Sigma}=\mathrm{diag}\left(\lambda_1,\lambda_2,\dots,\lambda_{N_\mathrm{t}}\right)\in\mathbb{C}^{N_\mathrm{t}\times N_\mathrm{t}}$ is a diagonal matrix whose diagonal contains the eigenvalues of matrix $\boldsymbol{\mathcal{A}}$ and the rest entries are all zeros. Correspondingly, the diagonal matrix $\left(\boldsymbol{\Sigma}+\lambda_\mathrm{opt}\mathbf{I}_{N_\mathrm{t}}\right)$ places the eigenvalues of matrix $\left(\boldsymbol{\mathcal{A}}+\lambda_\mathrm{opt}\mathbf{I}_{N_\mathrm{t}}\right)$ on its diagonal.

By defining the smallest eigenvalue of matrix $\boldsymbol{\mathcal{A}}$ as λ_min, we have the conclusion that $\lambda_\mathrm{opt}>-\lambda_\mathrm{min}$. By substituting (45) and (46) into the transmit power constraint $\|\mathbf{F}\|_F^2=P_T$, we have the following equation

$$\left\|\left(\boldsymbol{\mathcal{A}}+\lambda_{\text{opt}}\mathbf{I}_{N_\text{t}}\right)^{\dagger}\boldsymbol{\mathcal{B}}\right\|_F^2=\left\|\mathbf{V}\left(\boldsymbol{\Sigma}+\lambda_{\text{opt}}\mathbf{I}_{N_\text{t}}\right)^{-1}\mathbf{V}^{-1}\boldsymbol{\mathcal{B}}\right\|_F^2$$
$$=\left\|\mathbf{V}\left(\boldsymbol{\Sigma}+\lambda_{\text{opt}}\mathbf{I}_{N_\text{t}}\right)^{-1}\mathbf{V}^{H}\boldsymbol{\mathcal{B}}\right\|_F^2=\left\|\left(\boldsymbol{\Sigma}+\lambda_{\text{opt}}\mathbf{I}_{N_\text{t}}\right)^{-1}\mathbf{V}^{H}\boldsymbol{\mathcal{B}}\right\|_F^2$$
$$=\sum_{i=1}^{N_\text{t}}\frac{\|\mathbf{D}(i,:)\|^2}{\left(\lambda_{\text{opt}}+\lambda_i\right)^2}=P_T. \tag{47}$$

Where $\mathbf{D}=\mathbf{V}^H\boldsymbol{\mathcal{B}}$. Then we can construct a one-dimensional search problem as

$$\min_{\lambda_{\text{opt}}}\ \lambda_{\text{opt}}P_T+\sum_{i=1}^{N_\text{t}}\frac{\|\mathbf{D}(i,:)\|^2}{\left(\lambda_{\text{opt}}+\lambda_i\right)}\ . \tag{48}$$
$$\text{s.t.}\ -\lambda_{\min}<\lambda_{\text{opt}}<10$$

Here we can choose a suitable one-dimensional optimization method, such as Bisection method or Golden Section Search method [28] to solve (48), and then we can substitute λ_{opt} into (45) to obtain $\mathbf{F}_{\text{opt}}$. The low-complexity algorithm for JSC beamforming with total antenna array transmit power constraint is summarized in Algorithm 3.

Algorithm 3. A low-complexity algorithm to solve (36)

Input: $\mathbf{H}\in\mathbb{C}^{N_\text{U}\times N_\text{t}}$, $\mathbf{F}_{\text{rad}}\in\mathbb{C}^{N_\text{t}\times N_{\text{tar}}}$, P_T, $\eta\in[0,1]$
Output: $\mathbf{F}_{\text{opt}}\in\mathbb{C}^{N_\text{t}\times N_\text{U}}$
1: Construct $\mathbf{F}_0\in\mathbb{C}^{N_\text{t}\times N_\text{U}}$ by (37).
2: Construct $\mathbf{A}\in\mathbb{C}^{(N_\text{U}+N_\text{t})\times N_\text{t}}$ and $\mathbf{B}\in\mathbb{C}^{(N_\text{U}+N_\text{t})\times N_\text{U}}$, and construct $\boldsymbol{\mathcal{A}}=\mathbf{A}^H\mathbf{A}$ and $\boldsymbol{\mathcal{B}}=\mathbf{A}^H\mathbf{B}$.
3: Use Golden Section Search to solve (48), and obtain λ_{opt}.
4: Compute $\mathbf{F}_{\text{opt}}$ by (45).

On next stage, we consider JSC beamforming design with transmit power constraint on per antenna, similar to (36), we rewrite the weighted minimization problem as

$$\min_{\mathbf{F}}\ \eta\left\|\mathbf{HF}-\mathbf{I}_{N_\text{U}}\right\|_F^2+(1-\eta)\|\mathbf{F}-\mathbf{F}_0\|_F^2. \tag{49}$$
$$\text{s.t.}\ \text{diag}(\mathbf{FF}^H)=\frac{P_T}{N_\text{t}}\mathbf{I}_{N_\text{t}}$$

The corresponding $\mathbf{F}_0$ can be obtained via (37). Then we construct $\mathbf{A}\in\mathbb{C}^{(N_\text{U}+N_\text{t})\times N_\text{t}}$ and $\mathbf{B}\in\mathbb{C}^{(N_\text{U}+N_\text{t})\times N_\text{U}}$ again, and rewrite (48) as

$$\min_{\mathbf{F}}\ \|\mathbf{AF}-\mathbf{B}\|_F^2. \tag{50}$$
$$\text{s.t.}\ \text{diag}(\mathbf{FF}^H)=\frac{P_T}{N_\text{t}}\mathbf{I}_{N_\text{t}}$$

By temporarily ignoring the transmit power constraint on per antenna, and define $\mathbf{F}^H=\sqrt{\frac{P_T}{N_\text{t}}}\mathbf{F}_\text{B}\in\mathbb{C}^{N_\text{U}\times N_\text{t}}$, we can also rewrite (50) as

$$\min_{\mathbf{F}_\text{B}}\ \left\|\sqrt{\frac{P_T}{N_\text{t}}}\mathbf{F}_\text{B}\mathbf{A}^H-\mathbf{B}^H\right\|_F^2. \tag{51}$$
$$\text{s.t.}\ \text{diag}(\mathbf{F}_\text{B}^H\mathbf{F}_\text{B})=\mathbf{I}_{N_\text{t}}$$

The Euclidean gradient of the objective function in (51) can be calculated as $2\left(\sqrt{\frac{P_T}{N_\text{t}}}\mathbf{F}_\text{B}\mathbf{A}^H-\mathbf{B}^H\right)\sqrt{\frac{P_T}{N_\text{t}}}\mathbf{A}$.

Here we recommend the complex oblique manifold factory of MATLAB Manopt toolbox and Conjugate Gradient algorithm to solve (51) [29]. In order to guarantee the transmit power constraint on per antenna, the optimal digital beamforming matrix should be normalized as $\mathbf{F}_{\text{opt}}=\sqrt{\frac{P_T}{N_\text{t}}}\mathbf{F}_\text{B}^H$. And we summarize the low-complexity algorithm for JSC beamforming with per antenna transmit power constraint in Algorithm 4.

Algorithm 4. A low-complexity algorithm to solve (49)

Input: $\mathbf{H}\in\mathbb{C}^{N_\text{U}\times N_\text{t}}$, $\mathbf{F}_{\text{rad}}\in\mathbb{C}^{N_\text{t}\times N_{\text{tar}}}$, P_T, $\eta\in[0,1]$
Output: $\mathbf{F}_{\text{opt}}\in\mathbb{C}^{N_\text{t}\times N_\text{U}}$
1: Construct $\mathbf{F}_0\in\mathbb{C}^{N_\text{t}\times N_\text{U}}$ by (37).
2: Construct $\mathbf{A}\in\mathbb{C}^{(N_\text{U}+N_\text{t})\times N_\text{t}}$ and $\mathbf{B}\in\mathbb{C}^{(N_\text{U}+N_\text{t})\times N_\text{U}}$.
3: Compute $\mathbf{F}_\text{B}\in\mathbb{C}^{N_\text{U}\times N_\text{t}}$ by solving (51), and normalize as $\mathbf{F}_{\text{opt}}=\sqrt{\frac{P_T}{N_\text{t}}}\mathbf{F}_\text{B}^H$.

6 Simulation Results

6.1 Hybrid Beamforming Design Analysis for SU-MIMO JSC

In this section, we will test the performance of Algorithm 1 and Algorithm 2 via Monte-Carlo simulation. Assuming $N_\text{s}=10$ data streams at each subcarrier are sent from OFDM-JSC transmitter with $N_\text{t}=120$ antennas and $N_\text{RF}=20$ RF chains to a UE with $N_\text{r}=40$ receive antennas, while the discrete azimuth angles of directions which need to be detected are $[-45°, 0°, 45°]$, respectively. We set the average transmit power per subcarrier as $P_T=1\text{W}$. And the total number of subcarriers is $K=32$. In our simulation, the parameters related to channel model (3) are set as $N_\text{C}=5$ clusters with $N_\text{R}=10$ rays in each cluster. And the discrete azimuth AoAs and AoDs of each ray are generated through Laplacian distribution with mean cluster angles, which are independently and uniformly distributed over $\left[-\frac{\pi}{2},\frac{\pi}{2}\right]$. And the angular spread within each cluster is 10°. Note that we did not set a strong LOS propagation path here.

For simplicity in following simulation, let we use 'Optimal-FD' to represent the spectral efficiency of OFDM-JSC system with communication-only optimal fully digital beamformer. And the baseline radar beampattern is denoted by 'Radar-only'. Then we denote the beamforming design for OFDM-JSC transmitter with partially connected hybrid beamforming structure and fully connected hybrid beamforming structure as 'HBP' and 'HBF', respectively.

We first show the spectral efficiency of OFDM-JSC system in Figure 3. It can be observed that OFDM-JSC system will retain a poor communication performance when $\eta=0$, since at this time the beamforming in OFDM-JSC transmitter is only designed for radar sensing. By rising the value of weighting factor η, a larger weight is assigned to minimize the Euclidean distance between hybrid beamforming matrix and the optimal fully digital beamforming matrix, thus the spectral efficiency of OFDM-JSC system is also on the rise, and gradually approaching the optimal fully digital beamforming.

Through Figure 3, we can also observe that HBF-OFDM-JSC transmitter performs better than HBP-OFDM-JSC transmitter in spectral efficiency when the weighting factor $\eta > 0$. Especially when $\eta = 1$, the spectral efficiency of HBF-OFDM-JSC transmitter can almost approximate to the optimal fully digital beamforming, while there is still a significant gap in spectral efficiency between HBP-OFDM-JSC transmitter and the optimal fully digital beamforming. This is because that the HBF-OFDM-JSC transmitter is equipped with more phase shifters than the HBP-OFDM-JSC transmitter, which also brings higher hardware costs and higher energy consumption, especially in massive MIMO system.

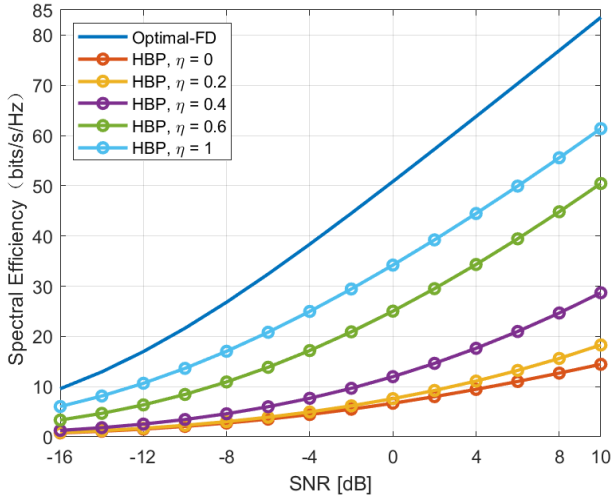

(a) Hybrid JSC beamforming achieved by Algorithm 1

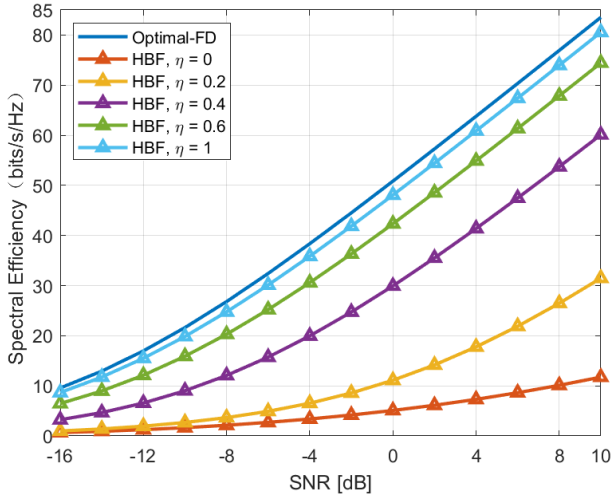

(b) Hybrid JSC beamforming achieved by Algorithm 2

Figure 3. Spectral efficiency vs SNR, when $\eta = 0, 0.2, 0.4, 0.6, 1$

Figure 4 shows the associated beampattern of OFDM-JSC transmitter. As we can observe that when $\eta = 1$, OFDM-JSC transmitter cannot point its beams toward the directions which need to be detected, since at this time the beamforming in OFDM-JSC transmitter is only designed for downlink communication. It needs to be emphasized that since we assume that UE is NLOS, OFDM-JSC transmitter will not directly point its beam directed at the UE even when $\eta < 1$. As the value of η increases, the weight assigned to downlink communication increases, while the weight assigned to radar sensing decreases accordingly, which will cause the beampattern of OFDM-JSC transmitter to gradually deviate from the baseline radar beampattern. The specific performance is that the main lobe gain gradually decreases, and the side lobe gain gradually increases, while the main lobes can still be aligned with the directions which need to be detected, thus ensuring a certain radar sensing performance. Through Figure 4. We can observe that when the weighting factor η is fixed, the beam width of HBF-OFDM-JSC transmitter is much narrower than that of HBP-OFDM-JSC transmitter, which also brings much higher main lobe gain. This is because that equipping fewer phase shifters limits the degrees of freedom (DOF) of beamforming design in HBP-OFDM-JSC transmitter.

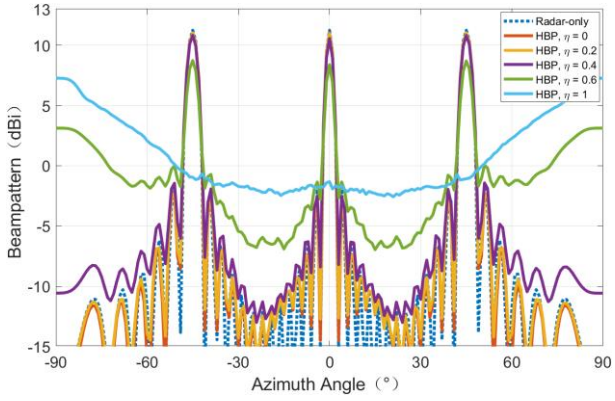

(a) Hybrid JSC beamforming achieved by Algorithm 1

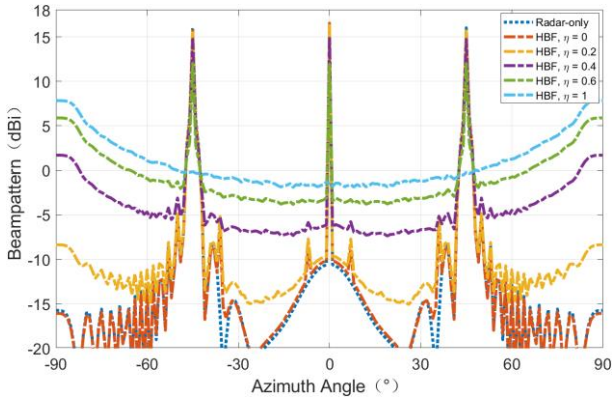

(b) Hybrid JSC beamforming achieved by Algorithm 2

Figure 4. Beampattern in azimuth plane, when $\eta = 0, 0.2, 0.4, 0.6, 1$

Then we reduce the number of antennas in HBF-OFDM-JSC transmitter as $N_t = 40$, and the corresponding simulation results are shown in Figure 5. The result is obvious that HBF-OFDM-JSC transmitter with $N_t = 40$ can achieve the same beam width as HBP-OFDM-JSC transmitter with $N_t = 120$. And we can also see that with different value of η, the spectral efficiency of HBF-OFDM-JSC transmitter with $N_t = 40$ is always higher than that of HBP-OFDM-JSC transmitter with $N_t = 120$. As we can summarize that, HBF structure can provide much higher downlink communication and radar sensing performance for OFDM-JSC system than HBP structure. The only advantage of HBP structure is its lower hardware cost, which will inevitably lead to performance loss.

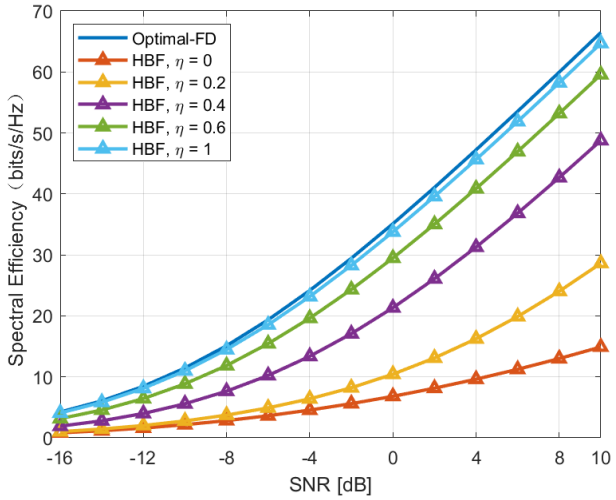

(a) Spectral efficiency vs SNR

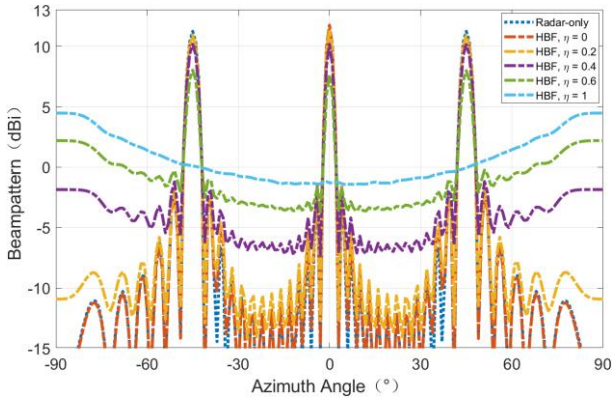

(b) Beampattern in azimuth plane

Figure 5. Hybrid JSC beamforming achieved by Algorithm 2, when $\eta = 0, 0.2, 0.4, 0.6, 1$ with $N_{\mathrm{t}} = 40$

6.2 Beamforming Design Analysis for MU-MISO JSC

In order to prove the effectiveness of proposed JSC beamforming design in MU-MISO scenario, we present numerical results in this section. In Monte-Carlo simulation, we set $N_{\mathrm{t}} = 20$ antennas equipped in JSC transmitter and the number of downlink single receive antenna UEs is set as $N_{\mathrm{U}} = 4$, the average transmit power is $P_T = 1\mathrm{W}$. And we set the discrete azimuth angles corresponding to directions which need to be detected as $[-45°, 0°, 45°]$, respectively, which means $N_{\mathrm{tar}} = 3$. Suppose that QPSK modulation is used in the JSC system. In channel model (35), the number of propagation paths from JSC to each UE is set as $N_{\mathrm{C}} = 10$, and the discrete azimuth AOD of each path are independently generated from uniform distributions over $\left[-\frac{\pi}{2}, \frac{\pi}{2}\right]$. For convenience in the following simulation, we use 'No MI' to represent the ideal situation in absence of multiuser interference. Further, we denote JSC beamforming design with total antenna array transmit power constraint and per antenna transmit power constraint as 'Total' and 'PerAnt', respectively.

We first show the spectral efficiency of JSC system in Figure 6(a). It can be observed that by setting $\eta = 0.4$, the downlink communication performance of JSC system will suffer a certain loss. As the value of weighting factor η increases, the spectral efficiency of JSC system is also on the rise and gradually approaching the ideal situation without multiuser interference, since greater weight has been assigned to downlink communication and the multiuser interference will be sufficiently suppressed.

Similar conclusions can also be drawn by analyzing the BER of JSC system, as shown in Figure 6(b). As the value of η increases, the bit error rate (BER) of JSC system drops rapidly, and can even reach the ideal situation without multiuser interference when η is large enough.

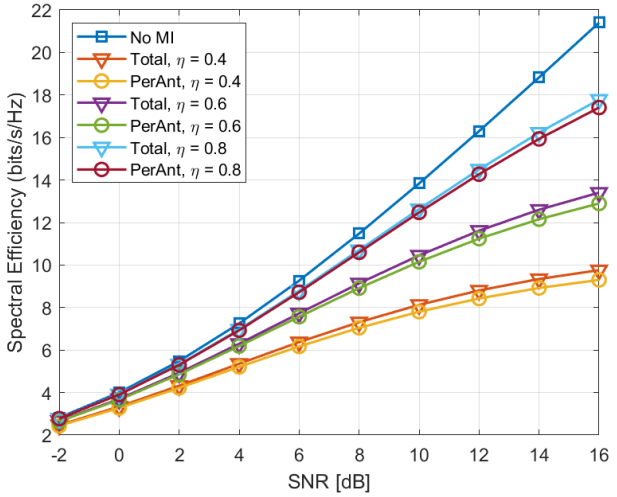

(a) Spectral efficiency vs SNR

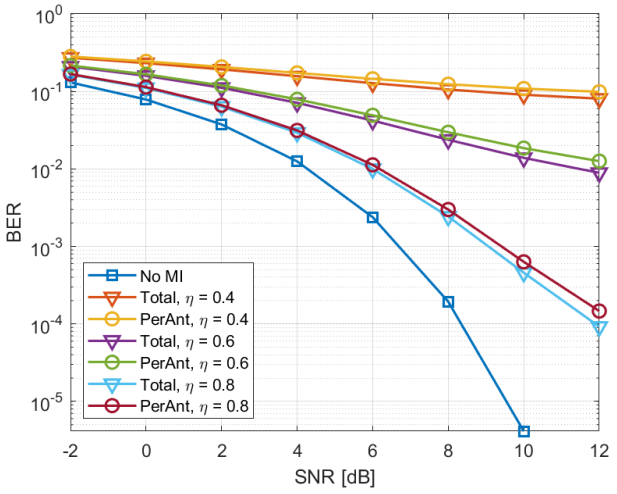

(b) Bit error rate vs SNR

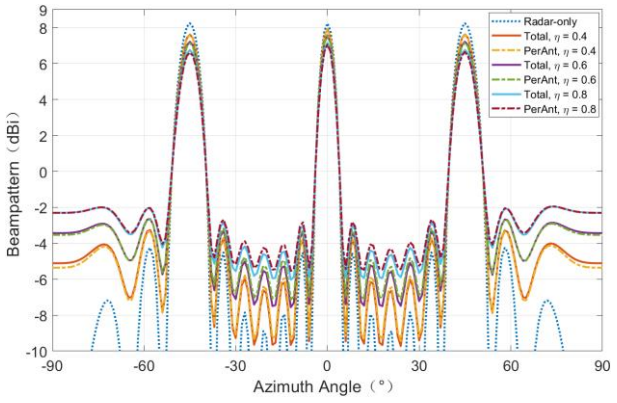

(c) Beampattern in azimuth plane

Figure 6. JSC beamforming achieved by Algorithm 3 and Algorithm 4, when $\eta = 0.4, 0.6, 0.8$

Figure 6(c) shows the associated beampattern of JSC transmitter. Similar to the SU-MIMO scenario we discussed in previous subsection, when the value of weighting factor η is on the rise, the transmit beampattern of JSC transmitter will gradually deviate from the baseline radar beampattern. The specific performance is that the main lobe gain gradually decreases, and the side lobe gain gradually increases, while the main lobes can still point to the specified directions which need to be detected, thus ensuring a certain radar sensing performance. It needs to be emphasized that although the JSC beamforming with total antenna array transmit power constraint and per antenna transmit power constraint can get similar downlink communication and radar sensing performance, the calculation complexity of Algorithm 4 is much higher than Algorithm 3.

7 Conclusion

In this paper, we investigate the beamforming design for OFDM-JSC system, which can simultaneously perform communication and sensing. And we considered hybrid beamforming structure and digital beamforming structure, which are equipped on JSC transmitter in SU-MIMO and MU-MISO scenarios, respectively. The spectral efficiency and beampattern of JSC system achieved by proposed beamforming methods are evaluated, and the simulation results show that our proposed beamforming design can provide excellent radar sensing and downlink communication performance for JSC system in both SU-MIMO and MU-MISO scenarios. More importantly, it enables JSC system to timely meet the changing communication and sensing requirements in practical application scenarios by properly adjusting the weighting factor, especially in internet of vehicles. In our future work, we will introduce mobile edge computing (MEC) to assist multiple JSC systems in beamforming, which will be called joint sensing, communication and computation (JSCC).

8 Acknowledgments

This work was supported in part by the National Natural Science Foundation of China under Grant No. 62171392 and No. 61871339, in part by the Natural Science Foundation of Fujian Province of China No. 2021J01004.

References

[1] X. Lin, J. Li, R. Baldemair, J.-F. T. Cheng, S. Parkvall, D. C. Larsson, H. Koorapaty, M. Frenne, S. Falahati, A. Grovlen, K. Werner, 5G New Radio: Unveiling the Essentials of the Next Generation Wireless Access Technology, *IEEE Communications Standards Magazine*, Vol. 3, No. 3, pp. 30-37, September, 2019.

[2] X. Zhang, J. Liang, N. Wang, T. Chang, Q. Guo, H. Cui, Broadband Millimeter-Wave Imaging Radar-Based 3-D Holographic Reconstruction for Nondestructive Testing, *IEEE Transactions on Microwave Theory and Techniques*, Vol. 68, No. 3, pp. 1074-1085, March, 2020.

[3] C. Sturm, W. Wiesbeck, Waveform Design and Signal Processing Aspects for Fusion of Wireless Communications and Radar Sensing, *Proceedings of the IEEE*, Vol. 99, No. 7, pp. 1236-1259, July, 2011.

[4] Y. Liu, G. Liao, Z. Yang, J. Xu, Design of integrated radar and communication system based on MIMO-OFDM waveform, *Journal of Systems Engineering and Electronics*, Vol. 28, No. 4, pp. 669-680, August, 2017.

[5] F. Liu, C. Masouros, Hybrid Beamforming with Sub-arrayed MIMO Radar: Enabling Joint Sensing and Communication at mmWave Band, *ICASSP 2019 - 2019 IEEE International Conference on Acoustics*, *Speech and Signal Processing (ICASSP)*, Brighton, United Kingdom, 2019, pp. 7770-7774.

[6] S. D. Liyanaarachchi, C. B. Barneto, T. Riihonen, M. Heino, M. Valkama, Joint Multi-User Communication and MIMO Radar Through Full-Duplex Hybrid Beamforming, *2021 1st IEEE International Online Symposium on Joint Communications & Sensing (JC&S)*, Dresden, Germany, 2021, pp. 1-5.

[7] F. Liu, C. Masouros, Joint Beamforming Design for Extended Target Estimation and Multiuser Communication, *2020 IEEE Radar Conference (RadarConf20)*, Florence, Italy, 2020, pp. 1-6.

[8] F. Liu, C. Masouros, A. Li, J. Zhou, L. Hanzo, Simultaneous target detection and multi-user communications enabled by joint beamforming, *2018 IEEE Radar Conference (RadarConf18)*, Oklahoma City, USA, 2018, pp. 0089-0094.

[9] P. Kumari, M. E. Eltayeb, R. W. Heath, Sparsity-aware adaptive beamforming design for IEEE 802.11ad-based joint communication-radar, 2*018 IEEE Radar Conference (RadarConf18)*, Oklahoma City, OK, USA, 2018, pp. 0923-0928.

[10] P. Kumari, N. J. Myers, S. A. Vorobyov, R. W. Heath, A Combined Waveform-Beamforming Design for Millimeter-Wave Joint Communication-Radar, *2019 53rd Asilomar Conference on Signals, Systems, and Computers*, Pacific Grove, CA, USA, 2019, pp. 1422-1426.

[11] M. Temiz, E. Alsusa, M. W. Baidas, A Dual-Functional Massive MIMO OFDM Communication and Radar Transmitter Architecture, *IEEE Transactions on Vehicular Technology*, Vol. 69, No. 12, pp. 14974-14988, December, 2020.

[12] M. Temiz, E. Alsusa, M. W. Baidas, Optimized Precoders for Massive MIMO OFDM Dual Radar-Communication Systems, *IEEE Transactions on Communications*, Vol. 69, No. 7, pp. 4781-4794, July, 2021.

[13] M. Temiz, E. Alsusa, M. W. Baidas, Optimized Precoders for Vehicular Massive MIMO RadCom Systems, *2021 Joint European Conference on Networks and Communications & 6G Summit (EuCNC/6G Summit)*, Porto, Portugal, 2021, pp. 574-579.

[14] X. Wang, Z. Fei, Z. Zheng, J. Guo, Joint Waveform Design and Passive Beamforming for RIS-Assisted Dual-Functional Radar-Communication System, *IEEE Transactions on Vehicular Technology*, Vol. 70, No. 5, pp. 5131-5136, May, 2021.

[15] Y. Liu, G. Liao, Y. Chen, J. Xu, Y. Yin, Super-Resolution Range and Velocity Estimations with OFDM Integrated Radar and Communications Waveform, *IEEE Transactions on Vehicular Technology*, Vol. 69, No. 10, pp. 11659-11672, October, 2020.

[16] N. Li, Z. Wei, H. Yang, X. Zhang, D. Yang, Hybrid Precoding for mmWave Massive MIMO Systems with

Partially Connected Structure, *IEEE Access*, Vol. 5, pp. 15142-15151, June, 2017.

[17] T. Lin, J. Cong, Y. Zhu, J. Zhang, K. B. Letaief, Hybrid Beamforming for Millimeter Wave Systems Using the MMSE Criterion, *IEEE Transactions on Communications*, Vol. 67, No. 5, pp. 3693-3708, May, 2019.

[18] D. Wilcox, M. Sellathurai, On MIMO Radar Subarrayed Transmit Beamforming, *IEEE Transactions on Signal Processing*, Vol. 60, No. 4, pp. 2076-2081, April, 2012.

[19] J. Tan, L. Dai, Delay-Phase Precoding for THz Massive MIMO with Beam Split, *2019 IEEE Global Communications Conference (GLOBECOM)*, Waikoloa Village, HI, USA, 2019, pp. 1-6.

[20] B. Wang, F. Gao, S. Jin, H. Lin, G. Y. Li, S. Sun, T. S. Rappaport, Spatial-Wideband Effect in Massive MIMO with Application in mmWave Systems, *IEEE Communications Magazine*, Vol. 56, No. 12, pp. 134-141, December, 2018.

[21] A. Goldsmith, S. A. Jafar, N. Jindal, S. Vishwanath, Capacity limits of MIMO channels, *IEEE Journal on Selected Areas in Communications*, Vol. 21, No. 5, pp. 684-702, June, 2003.

[22] O. E. Ayach, S. Rajagopal, S. Abu-Surra, Z. Pi, R. W. Heath, Spatially Sparse Precoding in Millimeter Wave MIMO Systems, *IEEE Transactions on Wireless Communications*, Vol. 13, No. 3, pp. 1499-1513, March, 2014.

[23] A. Hassanien, S. A. Vorobyov, Phased-MIMO Radar: A Tradeoff Between Phased-Array and MIMO Radars, *IEEE Transactions on Signal Processing*, Vol. 50, No. 6, pp. 3137-3151, June, 2010.

[24] J. C. Gower, G. B. Dijksterhuis, *Procrustes Problems*, Oxford University Press, 2004.

[25] X. Yu, J. -C. Shen, J. Zhang, K. B. Letaief, Alternating Minimization Algorithms for Hybrid Precoding in Millimeter Wave MIMO Systems, *IEEE Journal of Selected Topics in Signal Processing*, Vol. 10, No. 3, pp. 485-500, April, 2016.

[26] F. Sohrabi, W. Yu, Hybrid Analog and Digital Beamforming for mmWave OFDM Large-Scale Antenna Arrays, *IEEE Journal on Selected Areas in Communications*, Vol. 35, No. 7, pp. 1432-1443, July, 2017.

[27] L. Liang, W. Xu, X. Dong, Low-Complexity Hybrid Precoding in Massive Multiuser MIMO Systems, *IEEE Wireless Communications Letters*, Vol. 3, No. 6, pp. 653-656, December, 2014.

[28] W. Huyer, A. Neumaier, Global optimization by multilevel coordinate search, *Journal of Global Optimization*, Vol. 14, No. 4, pp. 331-355, June, 1999.

[29] N. Boumal, B. Mishra, P.-A. Absil, R. Sepulchre, Manopt, a matlab toolbox for optimization on manifolds, *Journal of Machine Learning Research*, Vol. 15, No. 1, pp. 1455-1459, 2014.

Biographies

Minggan Ye received his B.S. degree from JiMei University, Xiamen, China in 2020. He is currently pursuing the M.S. degree in circuit and system with Xiamen University. His research interests include Mmwave Communication and Integrated Sensing-and-Communication.

Wei Hu received his B.S. degree from Xiamen University, Xiamen, China in 2020. He is currently pursuing the M.S. degree in electronic communication engineering with Xiamen University. His research interests include Mmwave Communication and Integrated Sensing-and-Communication.

Yifeng Zhao received his B.S. degree in Communication Engineering in 2002, M.S degree in Electronic Circuit System in 2005 and Ph.D. degree in Communication Engineering in 2014 from Xiamen University. He is an assistant professor of Communication Engineering, Xiamen University, Xiamen, Fujian, China. His current research interests include Mmwave Communication, Massive MIMO and Machine Learning applied in wireless communication.

Lianfen Huang received her B.S. degree in Radio Physics in 1984 and PhD in Communication Engineering in 2008 from Xiamen University. She was a visiting scholar in Tsinghua University in 1997. She is a professor in the Department of Communication Engineering, Xiamen University, Xiamen, Fujian, China. Her current research interests include wireless communication, wireless network and signal process.

Zhiyuan Shi received his B.S. degree in radio physics in 1984, M.S. degree in radio electronics in 1991 from Xiamen University. He is a Professor in the Department of electronic engineering, Xiamen University, Xiamen, Fujian, China. His current research interests include wireless communication, circuit and system.